View metadata, citation and similar papers at core.ac.uk
brought to you by CORE
provided by University of Johannesburg Institutional Repository

Influence of laser heat input on weld zone width and fatigue performance of Ti-6Al-4V sheet

P M Mashinini [a*] and D G Hattingh [b]

[a] University of Johannesburg, Department of Mechanical and Industrial Engineering Technology, Johannesburg, South Africa

[b] Nelson Mandela University, Department of Mechanical Engineering, Port Elizabeth, South Africa

[*]Corresponding Author at: University of Johannesburg, Department of Mechanical and Industrial Engineering Technology, Johannesburg, South Africa.

Email: mmashinini@uj.ac.za

Abstract

During this study, the fatigue life of laser welded Ti6Al4V sheet was evaluated as a function of process heat input. Heat input was varied by manipulating laser power and welding travel speed and was categorised into three heat input ranges (Low = 40 to 60 J/mm; Medium = 65 to 120 J/mm and High = 160 to 230 J/mm)). Fatigue data was acquired from as-welded and polished specimens in order to study the effect of weld geometry resulting from a change in process parameters. Results showed that there was an increase in fatigue life for low heat input welds, mainly derived from the associated higher traverse speeds, demonstrating that laser power variation was not the sole determinant in fatigue life. A higher fatigue life and lower heat input relationship is related to the occurrence of a narrower fusion zone and increased weld zone hardness that corresponds with a lower heat input obtained from higher traverse speeds. Two predominant crack initiation mechanisms were observed; internal initiation from discontinuities that is related to inadequate optimisation of welding process parameters for the polished samples, while surface initiation occurred in the welded specimens, due to the stress concentration effect of the weld bead geometry. An increase in welding speed or decrease in laser power both led to a reduction in weld undercut or a lower stress concentration at the weld

toe. As expected the fatigue data for the polished samples showed a marked improvement in life and a reduction in scatter compared to the as-welded data.

***Keywords**:* laser beam welding; Ti-6Al-4V; traverse speed; heat input; fatigue life

---

1. Introduction

Ti-6Al-4V (ASTM Grade 5) is the most widely used two phase α-β titanium alloy and has a high strength-to-weight ratio [1]. It is typically used in applications that exploit its excellent corrosion resistance; wide continuous service temperature range, from cryogenic temperatures up to about 425ºC; and its biocompatibility. The corrosion resistance of Ti-6Al-4V is based on the existence of a continuous oxide layer which is formed spontaneously upon exposure to oxygen. It has excellent resistance to corrosion in marine conditions, making it a good choice for use in offshore and subsea oil and gas operations where seawater corrosion and weight are concerns. In Europe and North America, however, the aerospace industry represents about 60 percent of the demand for titanium alloys. Most titanium alloys can be fusion welded, with embrittlement through contamination with air and carbonaceous materials posing the greatest threat to successful fusion welding [2]. With more usage and increasing demand for Ti based alloy materials, there is a need for better understanding of the behaviour of welded Ti-6Al-4V alloy especially with respect to the dynamic performance of the welded components. This paper provides insight into the influence of varying process heat input on laser welded Ti6Al4V sheet performance under tension-tension fatigue loading conditions for both as-welded and smooth specimens.

The weldability of titanium alloys is usually assessed based on the static properties (yield and UTS), toughness and ductility of the weld as well as on the resulting fatigue performance of the welded joint. Laser beam welding (LBW) offers low distortion and good productivity,

allowing a large range of component configurations to be joined using different welding positions [2]. In addition, laser welding is known for producing 'keyhole' welds with a narrow heat-affected zone, compared with most other fusion techniques with exception of electron beam welding [3, 4].

Precision in alignment and cutting of the faying joint surfaces is important, as excessive clearance makes it difficult to avoid undercut and associated porosity [5] that can significantly reduce the overall static and dynamic performance of the joint. In this respect, Ion [6] suggests that machined edges with a gap no larger than 5% of the material thickness should be used in laser welding. This figure is in agreement with the results of Li et al [5] who found that a gap of 0.1mm gave minimum levels of porosity for their 1.6 mm Ti-6Al-4V sheet (gap ≈ 6% of the plate thickness).

Mechanical properties in the α-β Ti-6Al-4V titanium alloy depend on the relative amounts and distributions of the α and β phases. The microstructure and mechanical properties are controlled by thermomechanical processing and heat treatment and can be substantially altered by forging or heat treatment that occurs either above or below the β-transus temperature (~ 1000ºC in commercial Ti-6Al-4V alloys) [7]. Clearly, fusion welding can lead to a variety of microstructures that will reflect the non-equilibrium heat input (controlled by process parameters), cooling rates and any post-weld heat treatment. Cao and Jahazi [8] used a Nd:YAG laser operating at 2.5 kW to weld 1 mm and 2 mm sheets of Ti-6Al-4V alloy. The authors observed that the fusion zone was predominantly acicular α' martensite leading to an increase in hardness relative to the mill annealed parent plate. In this autogenous welding, underfill defects were observed on both top and root surfaces of the weld and the underfill depth increased with increasing welding speed. Some micro-porosity was observed in the 2 mm joints which led to a decreased joint ductility compared with the parent plate, although

strength levels were similar or higher. No solidification cracks were observed in the fusion zone but HAZ cracking was occasionally found.

Higher levels of joint efficiency were reported by Casalino, Mortello and Campanelli [9] in a study of 2 mm annealed Ti-6Al-4V sheet using Ytterbium continuous wave fibre laser welding. They noted that successful laser welding depends on stability of the keyhole behaviour as, if it collapses, the penetration depth is lower and gas bubbles are trapped in the weld pool, leading to porosity and lower mechanical properties. Process parameter optimisation (including shielding gas flow rate) is a basic requirement for keyhole stability. They obtained joint mechanical efficiency values of around 80% but with a corresponding decrease in ductility of 60% to 70%. This ductility loss has also been observed by other authors and arises from the high hardness of the α' martensite phase in the fusion zone [10] or from porosity [8].

Squillace et al [10] reported a study of 1.6 mm mill annealed Ti-6Al-4V sheets autogenously welded using a Nd:YAG laser. It was observed successful welds at various heat input ranges. There is an intermediate heat input regime where the weld underfill reaches a maximum and the authors noted that the fatigue life of the welds investigated is strongly influenced by the value of the underfill radius. The underfill results from the convex shape of the fusion zone that is essentially "a groove weld condition in which the weld face or root surface is below the adjacent surface of the base metal" according to AWS A3.0M/A3.0:2010 [11]. Squillace et al [10] observed that their fatigue fractures initiated and propagated near the lowest point of the underfill convexity at the interface between the fusion zone and the HAZ.

Balasubramanian et al [12] have also reported work on the fatigue behaviour of 5.4 mm plates of Ti-6Al-4V alloy. They presented the fatigue results in the form of applied initial stress

intensity factor against cyclic life and noted that the laser welding process gave better fatigue life than either electron beam welding or gas tungsten arc welding.

Thus, a significant amount of published work is available on the effect of laser welding process parameters on microstructure and hardness, but work on fatigue of laser welded Ti-6Al-4V titanium alloy is more limited and less capable of generalisation. The present paper reports the influence of heat input on weld zone width, mechanical properties and the stress-life (S-N) fatigue performance of 3 mm thick specimens of Ti-6Al4V titanium alloy in the mill annealed condition.

2. Experimental procedure and sample preparation

Mill annealed Ti-6Al-4V sheets, 110 mm x 477 mm x 3 mm, were welded in a full penetration butt weld configuration along the 477 mm side. Chemical composition of the sheet material used was: (wt.%) Al 6.25, V 4.04, Fe 0.19, C 0.018, N 0.008, 0 0.18 and balance Ti. The welding platform used for this research was a TRUMPF LASERCELL 1005 CO_2 laser (TLF laser) based at the National Laser Centre (NLC) in Pretoria. The platform allows for gas shielding of the weld area on both top and bottom side of the joint line. During welding oxygen levels were kept low by applying Argon shielding gas over both top and bottom of the weld. Weld surface oxidation was minimised through a prolonged exposure of the weld seam to Argon gas shielding at a flow rate of 25 l/min for 20 minutes after completion of the weld. Welds were made using laser power values in the range from 2.3 kW to 4.3 kW and by increasing welding traverse speeds from 1 m/min to 5 m/min. Table 1 shows the experimental process parameters for each weld coupon as well as the calculated heat input in J/mm.

Table 1: Weld parameters used to manufacture specimens.

Weld No.	Laser Power, P (kW)	Traverse speed, F(m/min)	Heat Input, Q_{in} (J/mm)
1	2,3	3,0	46
2	2,8	1,0	168
3	2,8	2,0	84
4	2,8	4,0	42
5	3,3	1,0	198
6	3,3	3,0	66
7	3,3	5,0	40
8	3,8	1,0	228
9	3,8	2,0	114
10	3,8	4,0	57
11	4,3	3,0	86

These process parameters were used to calculate the weld heat input as shown in equation 1 that was adopted from literature [13, 14]:

$$Q_{in} = \frac{Laser\ Power}{Traverse\ speed} = \frac{60P}{F} \qquad (1)$$

Where Q_{in} = Heat input (J/mm), P = Laser power (W) and F = Traverse speed (mm/min).

It is worth noting that the weld heat input is a function of laser power and traverse (welding) speed. (Increased welding speed therefore results in a reduced heat input). Additionally it is important to be aware that welding speed/heat input is related to cooling rate which is a main contributor to weld microstructure [15-18]. This paper will focus on the macrostructure and consideration of microstructural influences/effects will be limited as it is well-covered in previous studies and reference publications.

The welded plates were sectioned transverse to the welding direction in preparing test samples for tensile testing, hardness and macrostructure evaluation. The macrostructure samples were mounted, polished and etched using a solution of 2 ml HF (40%); 5 ml H_2O_2 (30%); and 10 ml H_2O for approximately 30 seconds. Mounted specimens were also used for

Vickers microhardness evaluation by applying a 0.5 kgf load for 15 seconds. Hardness profiles were determined from measurements taken from the hardness indentations which were spaced at intervals of 0.5 mm across the weld at mid-section. These hardness profiles were used to identify the influence of the laser welding heat input on the hardness values observed in the weld nugget. Eighteen fatigue specimens were prepared from each welded plate according to the ASTM E466 standard. These specimens were then subjected to fatigue cycling with a measured test frequency of 55 Hz in load control at R = 0.1, using an electromagnetic Zwick Roell Vibrophore fatigue testing machine. Two groups of fatigue specimens were prepared, representing the as-welded condition with only the sharp specimens edges smoothed off, and a polished condition in which all external welding features were removed by grinding and polishing. A stepwise fatigue testing technique [19] was used where the initial tests were performed using a maximum stress of 900 MPa, equivalent to about 90% of the parent plate tensile strength (see Table 2) and then the maximum stress was decreased in 50 MPa steps until run-out was achieved (defined here as a life > 5 x 10^6 cycles).

Table 2: Mechanical properties and fatigue strength of parent plate.

	UTS (MPa)	**Yield Strength (MPa)**	**Elong. (%)**
Tensile results	1017	998	20
Vickers Hardness (H_V)		325±12 H_V	
Fatigue strength at R = 0.1 1x 10^6 cycles		640 MPa	
Fatigue strength at R = 0.1 5 x 10^6 cycles		550 MPa	

3. Results

3.1 Macrostructure

The weld macrostructure was assessed after chemical etching of sections taken transverse to the weld seam in order to enable measurement of the width of the fusion zone at the mid-thickness of the plate, i.e. the region where peak hardness was recorded. This, in turn, allows determination of a relationship between weld traverse speed and weld fusion zone width, and

hence leads to assist with establishing a relationship between weld width (process) and fatigue strength (performance). Figure 1 shows that the increase in fusion zone width with increase in heat input.

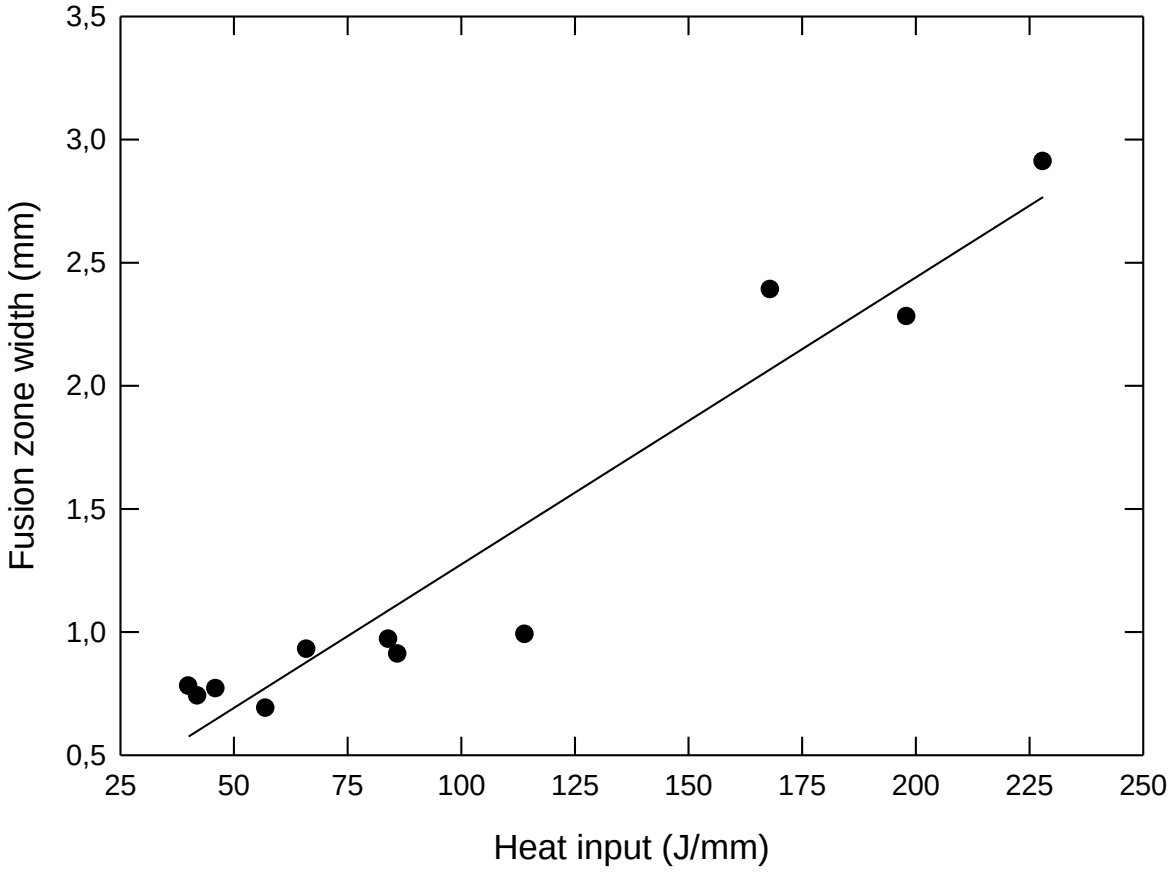

Figure 1: Weld fusion zone width as a function of heat input

Typical weld macrographs at low, medium and high heat input are illustrated in Figure 2 respectively. The images indicate that, as expected, weld zone width decreases with decrease in heat input. This is a similar trend to that reported by Hilton et al [20], Panwisawas et al. [21] and Junaid et al. [22], can be attributed to high conduction along the weld-line. The final weld geometry shows a similar "bell curve" appearance, with some decrease in thickness/weld undercut at the top and bottom of the weld. This variation in weld geometry will influence fatigue life in the as-welded specimens.

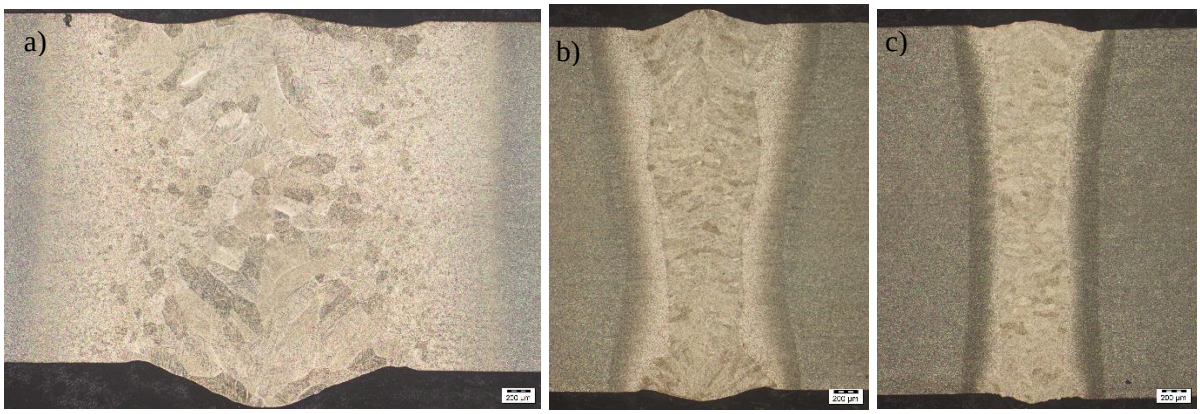

Figure 2: Typical macrographs at: a) high, b) medium and b) low heat input.

3.2 Micro hardness

The fusion zone hardness as a function of heat input is illustrated in Figure 3. The parent plate hardness was measured as 350 H_V and the high cooling rates associated with laser welding give rise to increase hardness in the fusion zone at every value of heat input used in this work. A linear relationship fits the results very well with a coefficient of determination or multiple regression (R^2) value of 0.997. The single exception to this linear relationship occurs at the lowest value of heat input of 40 J/mm and it is therefore likely that an additional microstructural effect is occurring at this heat input value. From the results in Figures 1 and 3, it is expected that Vickers hardness will also be related to weld width as is illustrated in Figure 4, and it can be seen that a linear relationship fits the data well (R^2 = 0.998), with the exception of two points. A quadratic equation fits the data less well (R^2 = 0.840). Finally, Figure 5 shows a plot of peak hardness in the weld fusion zone as a function of weld travel speed and it is again clear that a linear relationship provides a good fit to the data (R^2 = 0.997) with the exception of the point at the slowest travel speed and the highest heat input.

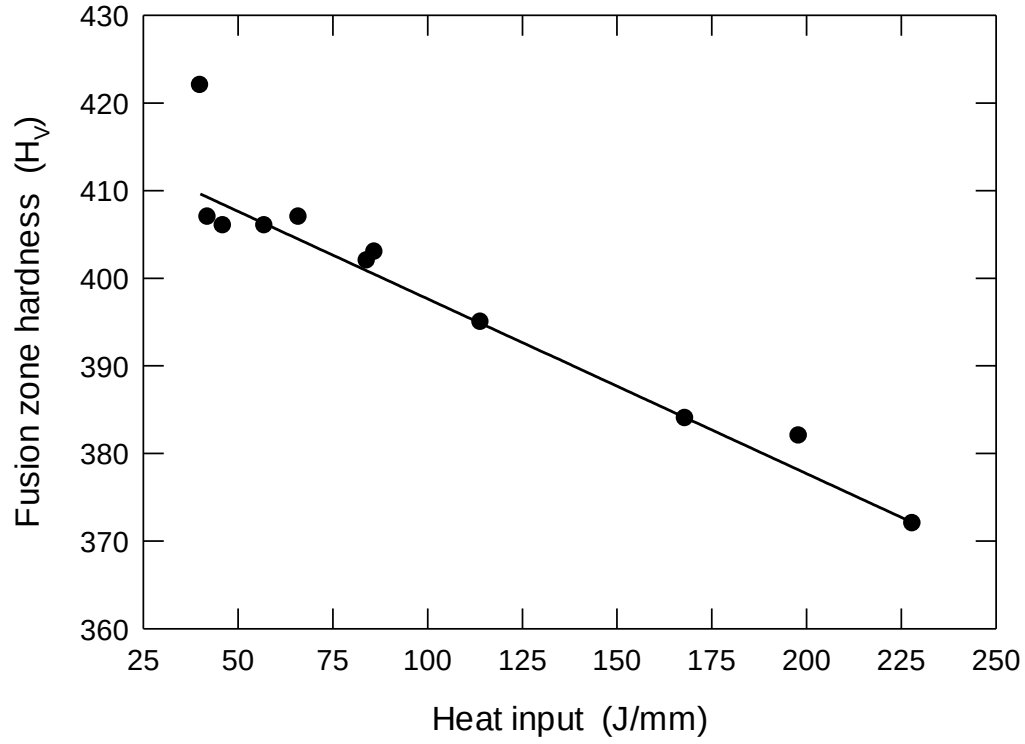

Figure 3: Peak hardness in the weld fusion zone as a function of heat input.

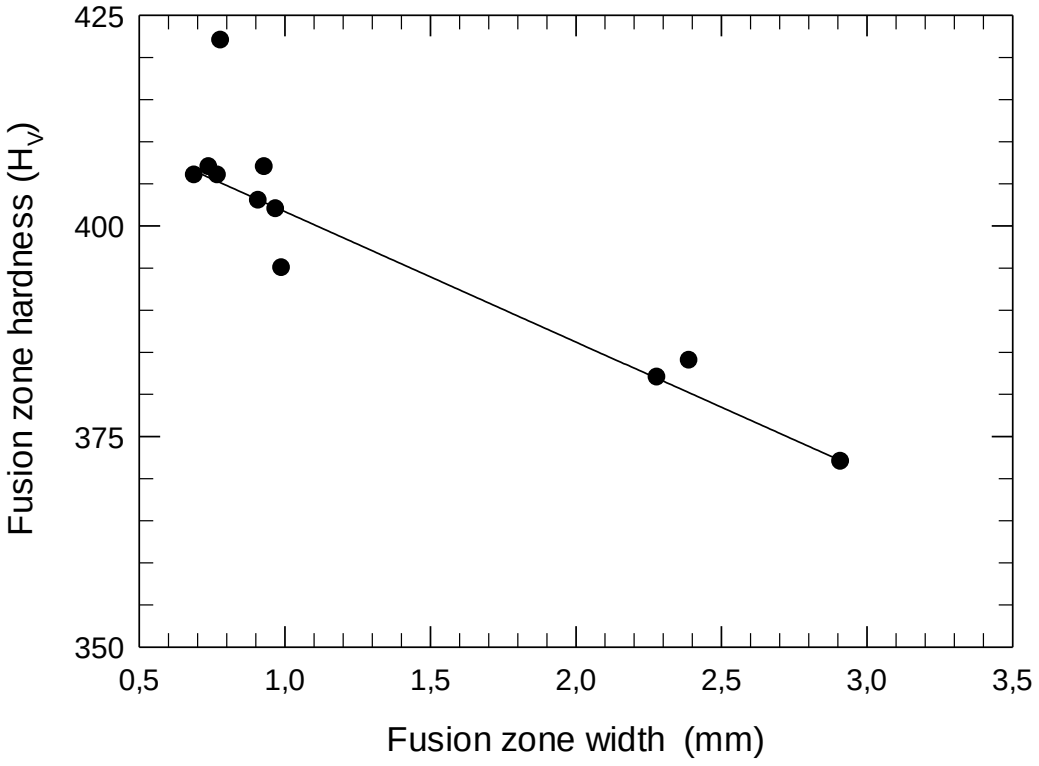

Figure 4: Peak hardness in the weld fusion zone as a function of fusion zone width.

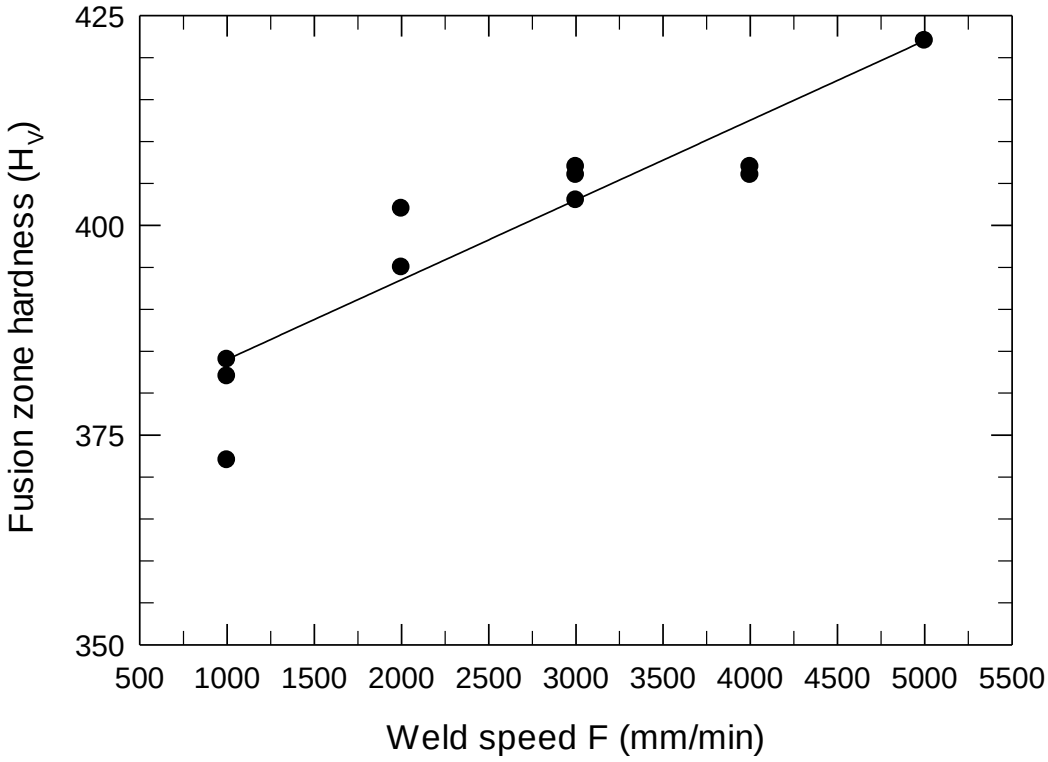

Figure 5: Peak hardness in the weld fusion zone as function of welding speed.

The conclusion is that fusion zone hardness is linearly related to heat input and to welding speed except at the lowest speed which is equivalent to the highest heat input. Heat input is the more fundamental parameter and it is reasonable to conclude that the hardness is generally related to the relative proportions of α and β-phases in the titanium alloy, although an additional effect is present at the highest heat input. So, hardness decreases as heat input goes up, which generally correlates with a decrease in weld travel speed.

3.3 Fatigue testing

Parent plate fatigue specimens were tested to establish a base-line curve for the alloy and to identify likely initial fatigue stresses to apply to laser welded specimens. The parent plate fatigue data is shown in Figure 6 and the fatigue strength at 5×10^5 cycles was observed to be around 550 MPa. Figure 6 also presents the fatigue data for the as-welded specimens and

it is clear that a large scatter band in the fatigue life is present. Plotting the fatigue data as a function of heat input bands, as seen in Figure 6, demonstrates that this achieves a reduction of the overall scatter band and it becomes clear that low heat input welds (40 – 57 J/mm, equivalent to higher hardness) tend to give a higher fatigue life than the welds made with either medium or high heat input. The high heat input welds (168 - 228 J/mm) generally give the lowest fatigue life at a given value of applied stress. Although there is insufficient data to draw accurate conclusions from regression lines fitted to the fatigue data in these heat input bands, there is an indication that the slopes of the regression lines vary between these heat input bands, which is a fairly common observation in as-welded specimens. The poorer fatigue performance observed at higher heat input levels is ascribed to the existence of weld undercut and its associated stress concentration, which is larger compared with the lower heat input welds. The highest fatigue strength observed at 5×10^6 cycles in the as-welded condition was 412 MPa achieved with a heat input of 57J/mm (low heat input).

Considering the fatigue data for the polished specimens shown in Figure 7, a considerable increase in fatigue performance is observed compared with the as-welded specimens, with the regression lines indicating fatigue strength values at 5×10^6 generally > 400 MPa, with the exception of the high heat input data. The parent plate regression line is also given in Figure 6 and it is apparent that the regression lines for the medium and low heat input specimens indicate a value of fatigue strength for these conditions at a cyclic life of 5×10^6 cycles within 50 MPa of the parent plate data. The net conclusion is that for these two sets of specimens welded with heat input values ranging from 66 – 228 J/mm, the increase in hardness observed in the fusion zone is largely able to offset any remaining effect of defects or detrimental microstructures in the HAZ or at the edge of the fusion zone. It is also clear from the regression lines, that fatigue strength is highest for the medium heat input welds (66 – 114 J/mm) than for the other two conditions. Figures 6 and 7 both indicate that welding has a significant influence on the fatigue

performance, compared with the parent plate. However, the change in slope of the S-N regression line data is relatively small in the case of polished specimens, except in the case of the low heat input tests. The as-welded specimens however show a very significant decrease in fatigue stress for equivalent lives, ranging for approximately 375 MPa for the low heat input to 200 MPa for the high input at a life of 10^5 cycles respectively. The conclusion for this data is that, provided the weld process conditions are correctly chosen (corresponding with a high heat input in the present case), laser beam welding is a very favourable joining process for welding 3 mm Ti-6Al-4V alloy sheets.

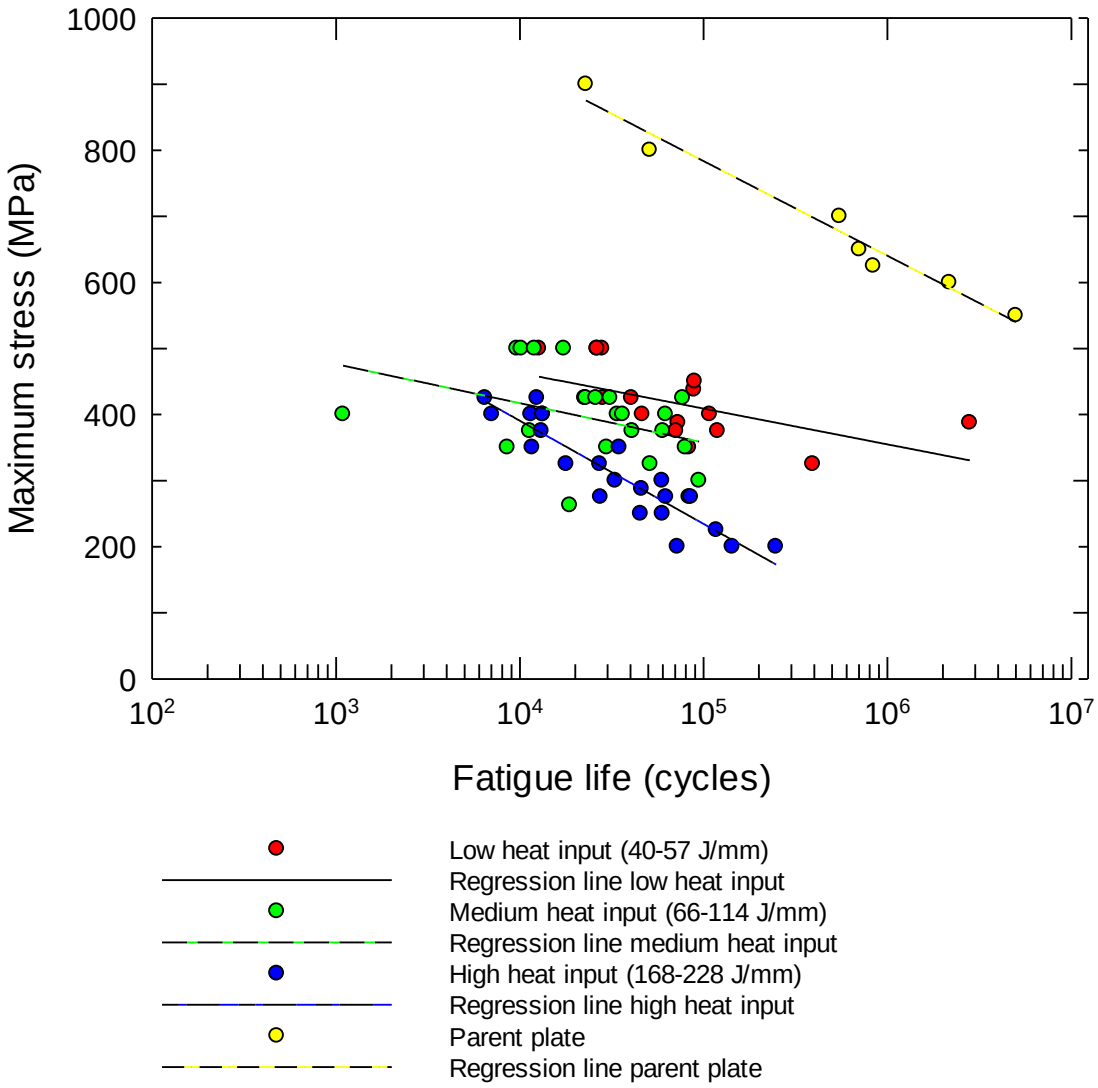

Figure 6: Fatigue data for as-welded specimens at all heat input levels. Data for unwelded parent plate specimens are also shown.

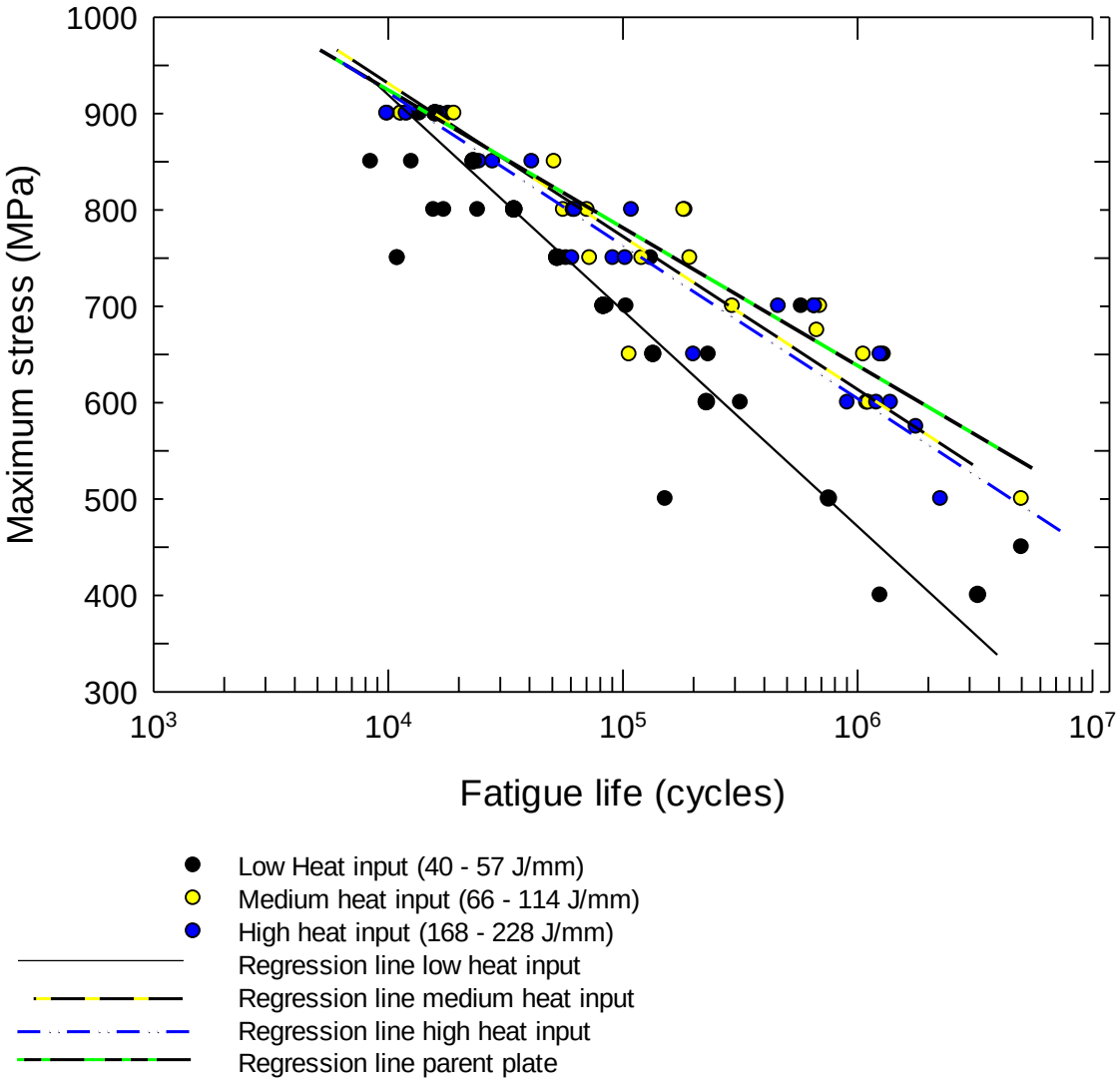

Figure 7: Fatigue data for specimens in the polished condition as a function of three heat input bands (low, medium and high). A regression line showing the parent plate fatigue data is also given.

3.4 Crack initiation sites

Fracture surfaces of specimens in both the as-welded and polished conditions were examined to identify the range of typical defects that were present. Fracture in the as-welded specimens predominantly initiated from the bottom (root) surface of the weld at the weld undercut (weld toe). The high local stress concentration leads to fast crack initiation and early growth and

hence to a reduced fatigue life. Figure 8 shows a typical example of the fracture surface of an as-welded specimen.

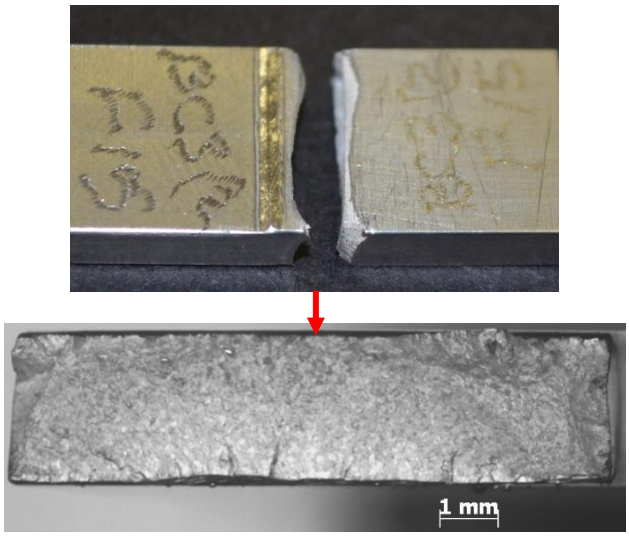

Figure 8: Representative macrograph of fracture surface of as-welded specimen that has failed at the weld toe.

The polished specimens showed improved fatigue life as geometrical notches at the edge of the fusion zone were largely eliminated by the polishing. Fatigue crack initiation generally occurred from internal voids in the fusion zone or from surface markings left from specimen preparation as polishing was only done up to 800 grit sandpaper. Figures 9 and 10 illustrate typical examples of fracture surfaces from polished specimens that illustrate both these modes of crack initiation. Void occurrence is associated with the high cooling rates associated with laser beam welding, which can lead to gas entrapment in the weld fusion zone [8]. Cao and Kahazi [23] also reported porosity in the weld zone similarly.

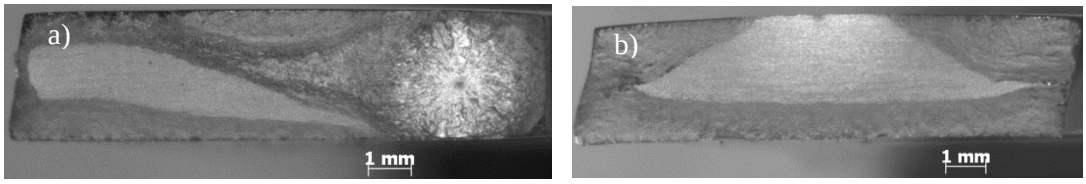

Figure 9: Representative macrographs of fracture surfaces for polished specimen that failed due to a) an internal void and b) polishing marks on the surface.

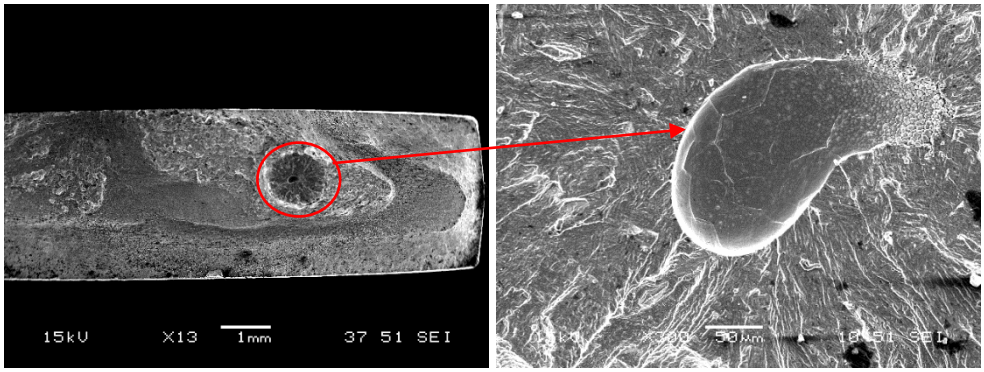

Figure 10: Fracture surface form a specimen welded with a heat input of 40 J/mm (3,300 W, 5 m/min), and tested in fatigue with R = 0.1 and a maximum stress of 850 MPa, which gave a life of 12,565 cycles. Initiation has occurred from a large region of gas porosity.

Figure 10 shows that such large regions of porosity readily initiate cracks. It was also observed that where specimens were cut from locations close to the stop-start positions in the weld, i.e. within perhaps 10 mm from the edge of the weld, this resulted in a very poor fatigue performance. In this case, evidence of the presence of smaller shrinkage cavities or porosity was observed with scanning electron microscopy (indicated in Figure 11) along with a more brittle appearance of the fracture surface.

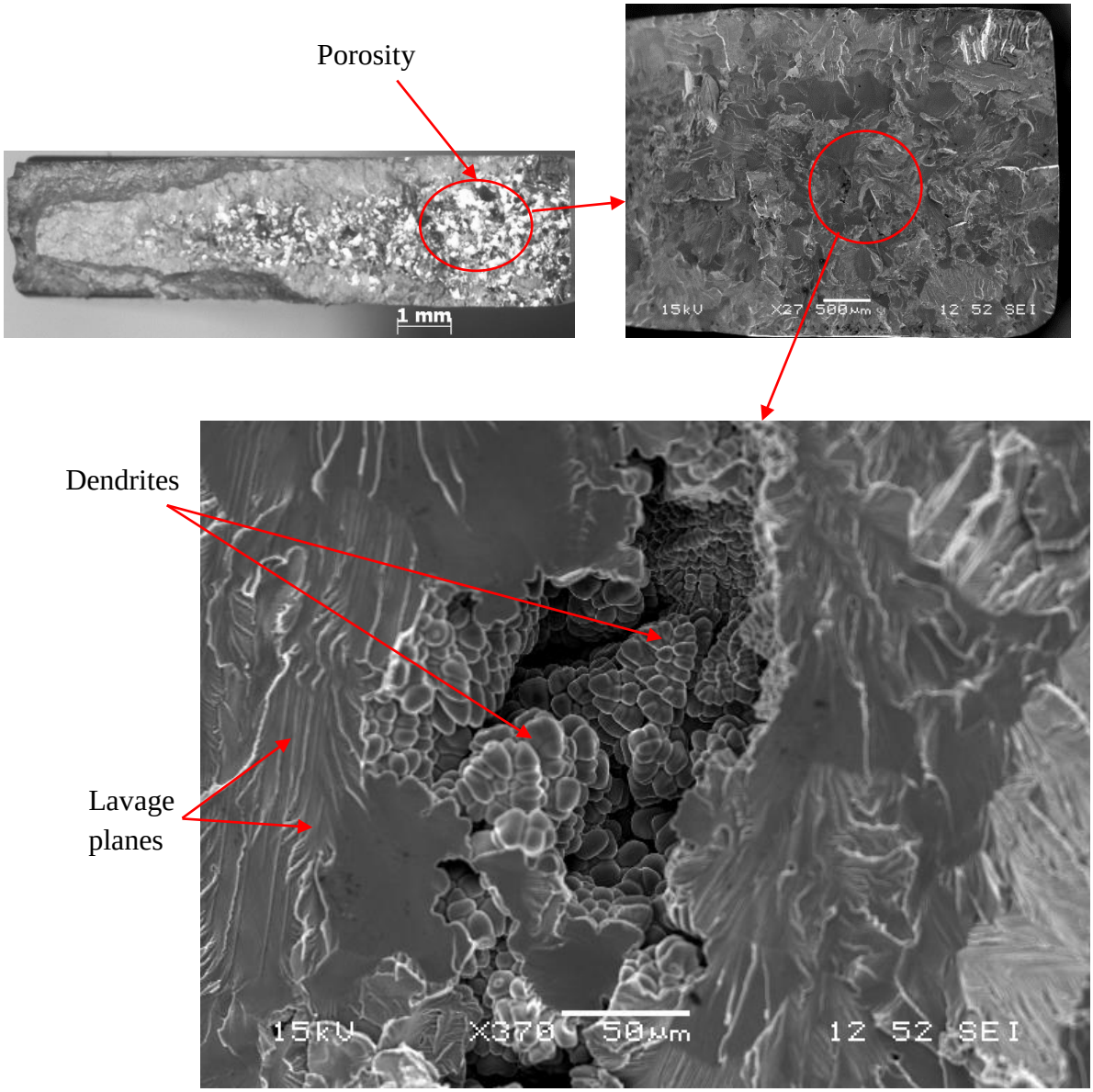

Figure 11: Typical fracture surface observed at a weld start/stop position; significant porosity is present.

4. Conclusion

This paper has demonstrated that in laser beam welding of 3mm Ti-6Al-4V alloy, the width of the weld fusion zone is mainly influenced by heat input, which is dependent to a first order on welding travel speed. Increase in welding speed resulted in a smaller fusion zone width. An increase in welding speed (largely equivalent to a reduction in heat input in this test programme) led to a reduction in width of the HAZ but an increase in Vickers hardness in the

fusion zone. Fatigue testing was carried out on specimens in the as-welded and polished condition. In the as-welded condition, fatigue life was influenced by increased welding speed which led to a greater degree of undercut (as observed in reference [8]). Specimen failure was predominantly due to geometrical features, such as undercut and porosity. Polishing the specimen increased the fatigue life at all lives. In the polished condition, the medium heat input specimens showed the best fatigue life for the weld process parameters used in this work. The majority of weld failures in the polished condition were influenced by the gas entrapment in the fusion zone as a result of the high cooling rates generally observed in laser welding and as well as cavity formation in the weld nugget.

Acknowledgements

The authors wish to express their thanks to the staff members from Nelson Mandela University Materials laboratory and National Laser Centre (NLC) situated at the Council for Scientific and Industrial Research (CSIR) and the National Department of Science and Technology for funding provided via the National Research Foundation (NRF) and TiCoC program, for supporting this research.

References

[1.] I.J. Polmear, 1 - The light metals, in: I.J. Polmear (Ed.) Light Alloys (Fourth Edition), Butterworth-Heinemann, Oxford, 2005, pp. 1-28.

[2.] T.I. Group, Welding Titanium: A Designers and Users Handbook, TWI, Great Abington, 1999.

[3.] J. Svenungsson, I. Choquet, A.F.H. Kaplan, Laser Welding Process – A Review of Keyhole Welding Modelling, Physics Procedia, 78 (2015) 182-191.

[4.] E. Akman, A. Demir, T. Canel, T. Sınmazçelik, Laser welding of Ti6Al4V titanium alloys, Journal of Materials Processing Technology, 209 (2009) 3705-3713.

[5.] Z. Li, S.L. Gobbi, I. Norris, S. Zolotovsky, K.H. Richter, Laser welding techniques for titanium alloy sheet, Journal of Materials Processing Technology, 65 (1997) 203-208.

[6.] J.C. Ion, Chapter 16 - Keyhole Welding, in: J.C. Ion (Ed.) Laser Processing of Engineering Materials, Butterworth-Heinemann, Oxford, 2005, pp. 395-455.

[7.] R. Wanhill, S. Barter, Metallurgy and Microstructure, in: Fatigue of Beta Processed and Beta Heat-treated Titanium Alloys, 2012, pp. 5-10.

[8.] X. Cao, M. Jahazi, Effect of welding speed on butt joint quality of Ti–6Al–4V alloy welded using a high-power Nd:YAG laser, Optics and Lasers in Engineering, 47 (2009) 1231-1241.

[9.] G. Casalino, M. Mortello, S.L. Campanelli, Ytterbium fiber laser welding of Ti6Al4V alloy, Journal of Manufacturing Processes, 20 (2015) 250-256.

[10.] A. Squillace, U. Prisco, S. Ciliberto, A. Astarita, Effect of welding parameters on morphology and mechanical properties of Ti–6Al–4V laser beam welded butt joints, Journal of Materials Processing Technology, 212 (2012) 427-436.

[11.] A.W. Society, AWS A3.0M/A3.0:2010 Standard WeldingTerms and Definitions, in, Miami, Florida, 2009, pp. 162.

[12.] T.S. Balsubramanian, V. Balasubramanian, M.A. Muthumanikkam, Effect of welding processes on fatigue properties of Ti-6Al-4V alloy joints, International Journal of Mechanical, Aerospace, Industrial, Mechatronic and Manufacturing Engineering, 5 (2011) 427-436.

[13.] Dawes C. Laser welding. ; 1992.

[14.] Hilton P. Nd: YAG laser welding. Cambridge, United Kingdom:; 2011.

[15.] Ahmed T, Rack HJ. Phase transformations during cooling in α+β titanium alloys. Materials Science and Engineering A243. 1998;(243): p. 206-211.

[16.] Kitamura K, Fujii H, Iwata Y, Sun YS, Morisada Y. Flexible control of microstructure and mechanical properties of friction stir welded Ti-6Al-4V joints. Materials and Design. 2013;(46): p. 348-354.

[17.] Xu P, Li L, Zhang S. Microstructure characterization of laser welded Ti-6Al-4V fusion zones. Material characterization. 2014; 87: p. 179-185.

[18.] Liu H, Nakata K, Yamamoto N. Microstructural characteristics and mechanical properties in laser beam welds of Ti6Al4V alloy. Material Science. 2012; 47: p. 1460-1470.

[19.] James MN, Hattingh DG, Bradley GR. Weld tool travel speed effects on fatigue life of friction stir welds in 5083 Aluminium. International Journal of Fatigue. 2003; 25(12): p. 1389-1398.

[20.] Hilton P, Blackburn J, Chong P. Welding of Ti-6Al-4V with fibre delivered laser beams. In International Congress on Applications of Lasers and Electro-Optics; 29 October - 1 November 2007; Orlando, United States of America.

[21.] Panwisawas C, Perumal B, Ward RM, Turner N, Turner RP, Brooks JW, Basoalto HC. Keyhole formation and thermal fluid flow-induced porosity during laser fusion welding in titanium alloys: Experimental and modelling. Acta Materialia. Vol. 126, March 2017, pages 251-263.

[22.] Junaid M, Khan FN, Rahman K, Baig NM. Effect of laser welding process on the microstructure, mechanical properties and residual stresses in Ti-5Al-2.5Sn alloy. Optics & laser Technology. Vol. 97, 1 December 2017, pages 405-419.

[23.] Cao X, Jahazi M. Effect of welding speed on butt joint quality of Ti–6Al–4V alloy welded using a high-power Nd:YAG laser. Optics and Lasers in Engineering. Vol. 47 (2009) 1231-1241.